

## Voyager Photometry of Iapetus

STEVEN W. SQUYRES

*Theoretical Studies Branch, NASA Ames Research Center, Moffett Field, California 94035*

BONNIE BURATTI

*NAS/NRC Research Associate, Jet Propulsion Laboratory, 4800 Oak Grove Drive,  
Pasadena, California 91109*

AND

JOSEPH VEVERKA AND CARL SAGAN

*Laboratory for Planetary Studies, Cornell University, Ithaca, New York 14853*

Received November 21, 1983; revised March 12, 1984

Voyager images of Iapetus ranging in phase angle from 8 to 90° were used to define the satellite's photometric properties and construct an albedo map of its surface. The images confirm that the albedo distribution has a roughly hemispheric asymmetry, as had been inferred from earlier analyses of the disk-integrated lightcurve. On the darker leading hemisphere albedo contours are roughly elliptical in shape and centered at the apex of orbital motion, flattened at the poles and elongated along the equator. The reflectance within the darker material is lowest (0.02-0.03) at the apex, and increases with increasing distance from the apex. The albedo pattern on the brighter trailing hemisphere is more complex. Reflectance increases gradually with increasing distance from the interface with the darker material, and reaches a maximum near the poles. Reflectances of 0.3-0.4 in the brighter material are common, and the highest values probably reach 0.6. The transition in reflectance contours between the two materials is gradual rather than sharp, and albedo histograms of images centered on the visually perceived boundary are weakly bimodal. The dark material on Iapetus is reddish, the bright material somewhat less so.

### INTRODUCTION

Since its discovery by Cassini in 1671, Saturn's satellite Iapetus has been known to exhibit some of the most unusual photometric properties in the solar system. Iapetus' leading hemisphere is among the darkest surfaces in nature, while parts of its trailing hemisphere are nearly as bright as snow. A variety of models has been proposed to account for this appearance (Cook and Franklin, 1970; Soter, 1974; Squyres and Sagan, 1983; Cruikshank *et al.*, 1983). With the acquisition of Voyager images (Fig. 1), it is possible to characterize the photometric properties of the surface of Iapetus in some detail. In this paper we use Voyager

data to investigate the albedo distribution, photometric function, and color of Iapetus.

Table I lists the Voyager images used in this study. They range in phase angle from 8 to 90°. We have worked primarily with Voyager 2 narrow angle camera images, which provide the highest resolution, in order to minimize the uncertainties that result from differences in calibration among cameras. All of the photometric quantities quoted here incorporate the calibration correction factors published by Danielson *et al.* (1981). For general characterization of the surface photometric properties we have used images obtained through the clear filter, which is centered near 0.47  $\mu\text{m}$  and extends from 0.31 to 0.65  $\mu\text{m}$  (Squyres and

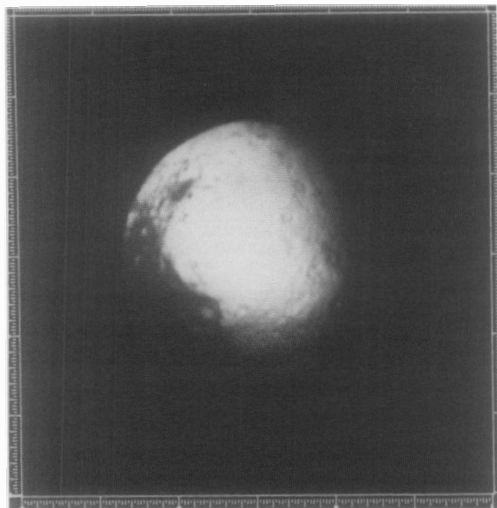


FIG. 1. A Voyager 2 narrow angle camera image of Iapetus (FDS 43894.24, clear filter).

Veveřka, 1981, Fig. 1). For color photometry, we have used images obtained through the narrow passband Voyager violet and orange filters, centered near 0.4 and 0.6  $\mu\text{m}$ , respectively.

Earth-based observations of Iapetus have been reviewed most recently by Cruikshank *et al.* (1983). Based on available data, the mean opposition magnitude of the dark leading hemisphere can be taken to be  $V_0 =$

$12.1 \pm 0.1$ . Using a radius of  $R = 730 \pm 20$  km (Smith *et al.*, 1981), one finds an average geometric albedo of  $p_v = 0.08 \pm 0.01$  for the dark leading hemisphere. Since the lightcurve amplitude reported for Iapetus averages  $1.8 \pm 0.1$  mag, corresponding to a brightness difference of a factor of 5.3, the average geometric albedo of the bright trailing hemisphere is  $p_v = 0.42 \pm 0.05$ . The leading hemisphere is distinctly redder than the trailing hemisphere. From the data summarized by Cruikshank (1979) the differences ( $\Delta = \text{Leading} - \text{Trailing}$ ) are  $\Delta(U - B) = 0.09 \pm 0.06$  and  $\Delta(B - V) = 0.09 \pm 0.03$ . Water ice features have been detected in the near-IR spectra of the bright hemisphere; spectra of the dark material are similar to those of extracts from tarry carbonaceous meteorites such as Murchison (Cruikshank *et al.*, 1983).

#### VOYAGER CLEAR FILTER OBSERVATIONS

Given the large variation of albedo over the surface of Iapetus and the limited imaging coverage obtained by Voyager, it is not possible to completely derive the photometric scattering properties of individual surface areas on the satellite. This situation arises because for no individual area on the satellite is coverage available over a significant range of incidence and emission angles at any particular phase angle. Thus one cannot carry out direct tests of the scattering laws as was done in the cases of Gany-mede and Callisto, for example, by Squyres and Veveřka (1981).

We will argue that all the available data for the dark material are consistent with a scattering law that is essentially lunar-like and that can be expressed by

$$I(i, \epsilon, \alpha) = F \left( \frac{\mu_0}{\mu_0 + \mu} \right) f(\alpha) \quad (1)$$

where  $i$  = incidence angle,  $\epsilon$  = emission angle,  $\alpha$  = phase angle,  $\mu = \cos \epsilon$ ,  $\mu_0 = \cos i$ ,  $I$  = intensity of scattered sunlight,  $\pi F$  = incident solar flux at  $i = 0$ , and  $f(\alpha)$  = phase function of the surface (Hapke, 1963; Ir-

TABLE I  
IMAGES USED

FDS No.	Phase angle ( $^\circ$ )	Camera	Filter	Subspacecraft longitude ( $^\circ$ )
43816.10	20	V2/NA	Clear	169
43851.55	23	V2/NA	Clear	179
43875.11	31	V2/NA	Clear	192
43886.17	39	V2/NA	Clear	203
43894.24	48	V2/NA	Clear	217
43907.08	68	V2/NA	Clear	261
43914.03	81	V2/NA	Clear	290
43918.43	90	V2/NA	Clear	305
43851.27	23	V2/NA	Violet	179
43851.39	23	V2/NA	Orange	179
43894.32	48	V2/NA	Violet	217
43894.40	48	V2/NA	Orange	217
43913.39	81	V2/NA	Violet	288
43913.47	81	V2/NA	Orange	288
34976.58	14	V1/NA	Clear	17
34951.56	8	V1/NA	Clear	3

TABLE II  
POINTS SAMPLED

Point	Latitude (°)	Longitude (°)	Material classification
A	9	264	Dark
B	8	223	Dark
D	32	179	Dark
E	40	163	Dark
F	6	180	Dark
G	10	150	Dark
H	43	129	Dark
N	17	166	Dark
P	32	151	Dark
R	-9	165	Dark
S	33	182	Dark
U	12	224	Dark
V	-6	234	Dark
W	9	213	Dark
X	17	194	Dark
O	46	226	Bright
Q	66	193	Bright
I	46	250	Bright
J	64	227	Bright
K	34	267	Bright
L	33	212	Bright
M	79	195	Bright
Y	27	241	Bright
Z	56	160	Bright
AA	25	204	Bright
BB	3	244	Bright
CC	48	140	Bright
DD	29	242	Bright

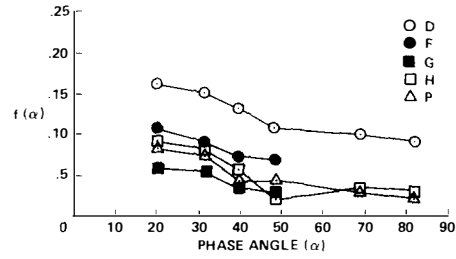


FIG. 2. Curves of  $f(\alpha)$  for five regions of dark material on Iapetus (see Eq. (1)).

photometric study (Table II). Among these are seven that lie well away from the dark terrain/bright terrain “boundary,” and that appear in up to five Voyager 2 clear filter images covering a range in phase angles from 20 to 81°. Areas sampled were centered on these points and typically covered  $5 \times 5$  picture elements (pixels). Because the photometric function of Eq. (1) can depart from observations very close to the terminator or limb, points in such locations were avoided. Using the measured reflectances and Eq. (1), curves of  $f(\alpha)$  over the range 20–81° were determined (Fig. 2). The curves may be averaged to give a mean  $f(\alpha)$  curve for Iapetus dark material, shown as the dashed curve in Fig. 3.

vine, 1966). Equation (1) has been shown to fit a wide variety of low albedo objects, including the Moon (Hapke, 1963), Phobos and Deimos (Noland and Veverka, 1977a,b; Klaasen *et al.*, 1979), and Callisto (Squyres and Veverka, 1981), and even bodies as bright as Ganymede (Squyres and Veverka, 1981). Only for very bright objects such as Europa (Buratti and Veverka, 1983) does this function not provide a satisfactory fit to Voyager observations. It is therefore appropriate as an approximation for the dark material on Iapetus. With this assumption, the phase function  $f(\alpha)$  for the dark material may be determined from observations that span a range of phase angles.

A total of fifteen points within the dark material have been selected for detailed

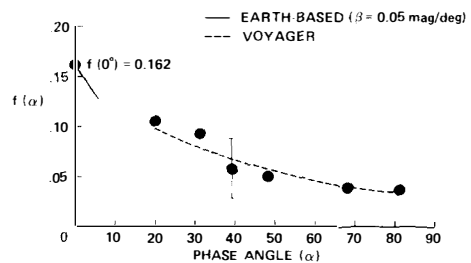


FIG. 3. Averaged  $f(\alpha)$  curve for dark material. The dashed curve from  $\alpha = 20^\circ$  to  $\alpha = 81^\circ$  was obtained by normalizing all curves to the mean  $f(\alpha)$  at  $\alpha = 48^\circ$  and averaging. Typical error bar shown is one standard deviation. The solid line from  $\alpha = 0^\circ$  to  $\alpha = 6^\circ$  is an extrapolation of our curve based on Earth-based observations summarized by Cruikshank (1979). Because of the paucity of data points, we have simply drawn this segment as a straight line with the appropriate mean slope.

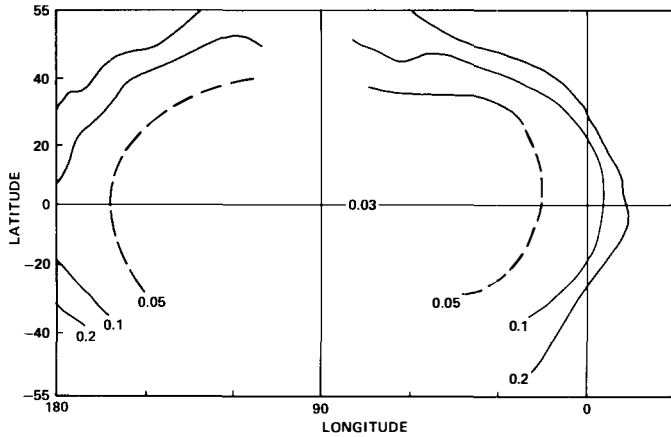


FIG. 4. Reflectance contours in the dark material from two Voyager clear filter images: FDS 43816.10 and FDS 34976.58. Contours give  $(I/F)/[\mu_0/(\mu_0 + \mu)]$ , normalized to a phase angle of  $20^\circ$  (i.e.,  $f(20^\circ)$ ). To convert to approximate normal reflectances, multiply by 0.8.

The Earth-based data are scaled to an average normal reflectance given by  $f(0^\circ)/2 = 0.08$  determined from Earth-based measurements of  $V_0$  and the radius found by Voyager. The slope of the phase curves near opposition (phase coefficient  $\beta = 0.05$  mag/deg) is based on the results of telescopic observations by a number of observers (summarized by Cruikshank, 1979), allowing for the fact that we are dealing with disk-resolved and not disk-integrated observations.

Using the data in Fig. 3 one can derive an approximate phase integral for the dark material on Iapetus. We find a phase integral  $q \approx 0.6$ , in accord with the radiometric results of Morrison (1977).

Using the photometric function of Eq. (1), it is also possible to produce a map giving the distribution of reflectance within the dark terrain, shown in Fig. 4. The contours give the quantity  $(I/F)/[\mu_0/(\mu_0 + \mu)]$  determined from two narrow angle clear filter images, one acquired by Voyager 1 and one by Voyager 2. The images used were acquired at different phase angles, and were corrected to  $\alpha = 20^\circ$  using the mean  $f(\alpha)$  curve for dark material given in Fig. 3.

The most noteworthy characteristic of this map is that the reflectance contours are

arranged concentrically about the apex of orbital motion. Iapetus is darkest at its apex, and becomes gradually brighter outward from the apex. The reflectance within the "dark material" actually varies by at least a factor of 3. The contours are not circular, but are roughly elliptical, being flattened at the poles and elongated along the equator.

Because no Voyager images in which dark material is clearly resolved exist for phase angles less than  $20^\circ$ , it is not possible to determine true normal reflectances for the dark material. Noting, however, that  $(I/F)/[\mu_0/(\mu_0 + \mu)]$  at  $\alpha = 0^\circ$  is twice the normal reflectance, and extrapolating from  $\alpha = 20^\circ$  to  $\alpha = 0^\circ$  on the basis of the Earth-based data in Fig. 3, the values in Fig. 4 may be converted to approximate normal reflectances by multiplying by a factor of 0.8. The area near the apex of orbital motion on Iapetus is among the darkest known surfaces in the solar system: the lowest reflectances exceed 1% but are probably less than 4% (see below). No bright "spots" or "islands" exist deep within the dark material.

We now turn to the photometric properties of the bright material. Our approach to dealing with this material is of necessity

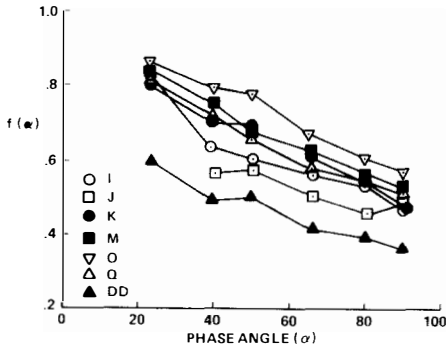


FIG. 5. Curves of  $f(\alpha)$  for seven regions of bright material on Iapetus.

somewhat different. From Earth-based observations we know that the geometric albedo of much of the bright material is at least 0.4, and higher values must occur given the albedo variation across the trailing hemisphere. In view of these higher albedos one needs to worry about the applicability of Eq. (1) to the scattering properties of the brighter material on Iapetus. The experience of Squyres and Veverka (1981), Buratti and Veverka (1983), and Buratti (1983) is helpful here. These studies show that for the icy satellites of Jupiter and Saturn Eq. (1) is a valid photometric law until reflectances in excess of about 0.6 are reached. As we shall see, most (and perhaps all) of the areas of Iapetus are below this limit. Hence, if the accumulated experience with other icy satellites can be extended to Iapetus, Eq. (1) can be used safely to deal with the brighter hemisphere of the satellites.

We have already stressed that coverage is too limited in  $i$  and  $\epsilon$  to test the applicability of Eq. (1) in a meaningful way for individual areas. It is also difficult to carry out such a test by grouping individual areas (on the basis of similar reflectance) due to the strong albedo variations that occur across the trailing hemisphere. Given the limited photometric coverage and large differences in apparent brightness it is difficult to know a priori how to select areas of "similar albedo." Nevertheless, when such tests are

attempted, the result is that an equation of the form

$$I(i, \epsilon, \alpha) = F \left( \frac{\mu_0}{\mu_0 + \mu} \right) f(\alpha) (A) + (1 - A)\mu_0 \quad (2)$$

can be fitted to the data, and that fits with  $A = 1.0$  are as good or better than for any other values of this parameter in the range from 0.0 to 1.0 (cf. Buratti, 1983). Thus we conclude that the Voyager data for the bright hemisphere of Iapetus can be analyzed using Eq. (1), and proceed on the basis of this conclusion. This of course does not mean that Eq. (1) fits the data uniquely and that other, more complex theoretical treatments are not useful, but merely that Eq. (1) provides an adequate description for our purposes.

A total of thirteen points in the bright material were selected for detailed study (Table II). The resulting  $f(\alpha)$  curves for some of these are shown in Fig. 5. The curves have a reasonably smooth appearance, consistent with the idea that Eq. (1) is a valid photometric function. The  $f(\alpha)$  curves for points in the bright material can be averaged (Fig. 6) to give a mean  $f(\alpha)$  curve that can be compared with Earth-based results. In Fig. 6 the Earth-based observations were drawn to have a normal reflectance  $f(0^\circ)/2$

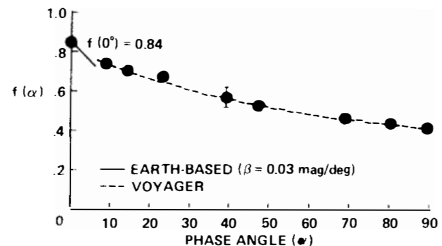


FIG. 6. Averaged  $f(\alpha)$  curve for bright material. Typical error bar shown is one standard deviation. The solid line from  $\alpha = 0^\circ$  to  $\alpha = 6^\circ$  is an extrapolation of our curve based on Earth-based observations summarized by Cruikshank (1979) and scaled to a bright material geometric albedo of 0.42. Because of the paucity of data points we have simply drawn this segment as a straight line with the appropriate mean slope.

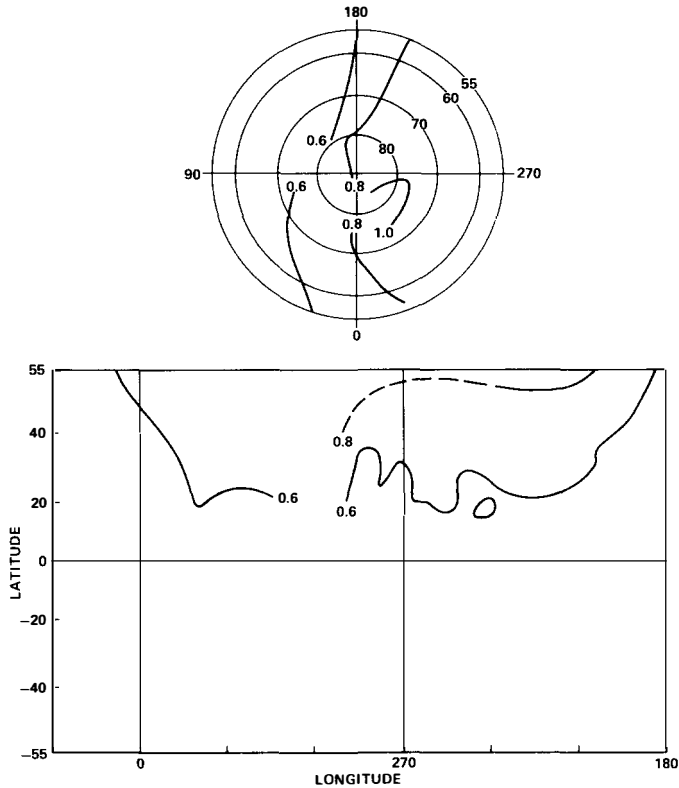


FIG. 7. Reflectance contours in the bright material from two Voyager clear filter images: FDS 43907.08 and FDS 34976.58. Contours give  $(I/F)/[\mu_0/(\mu_0 + \mu)]$ , normalized to a phase angle of  $20^\circ$  (i.e.,  $f(20^\circ)$ ). To convert to approximate normal reflectances, multiply by 0.65.

= 0.42, and a phase coefficient near opposition of  $\beta = 0.03$  mag/deg, consistent with the Earth-based data (summarized by Cruikshank, 1979). Note that since the points in Table II were not chosen in any systematic fashion the mean  $f(\alpha)$  curve does not represent exactly the average value for the bright hemisphere, and hence cannot be compared precisely with the Earth-based measurements.

Using the data in Fig. 6 we can derive an approximate phase integral for the bright material on Iapetus. We find  $q \approx 0.9$ , consistent with values for other saturnian satellites have reflectances in the range of those found on the trailing hemisphere of Iapetus, but difficult to reconcile with the value of 1.3 reported by Morrison *et al.* (1975).

Figure 7 shows a map of reflectance in

the bright material with the photometric function of Eq. (1) removed. As in Fig. 4, the values are correct for a phase angle of  $20^\circ$ . Some of the smaller details of the contour shapes may be related to topographic shading rather than actual albedo variations. The reflectance increases gradually with increasing distance from the apex of orbital motion. The reflectance varies by roughly a factor of 3 within the area sampled. There was no imaging of the antapex adequate for us to determine the reflectance there, but the general trend of the contours suggests strongly that Iapetus is brightest near the poles, rather than at the antapex.

In Fig. 8 we have combined the data from the leading and trailing hemispheres to produce an albedo map of Iapetus. Contours give the value of  $f(20^\circ)/2$ . Our map is quali-

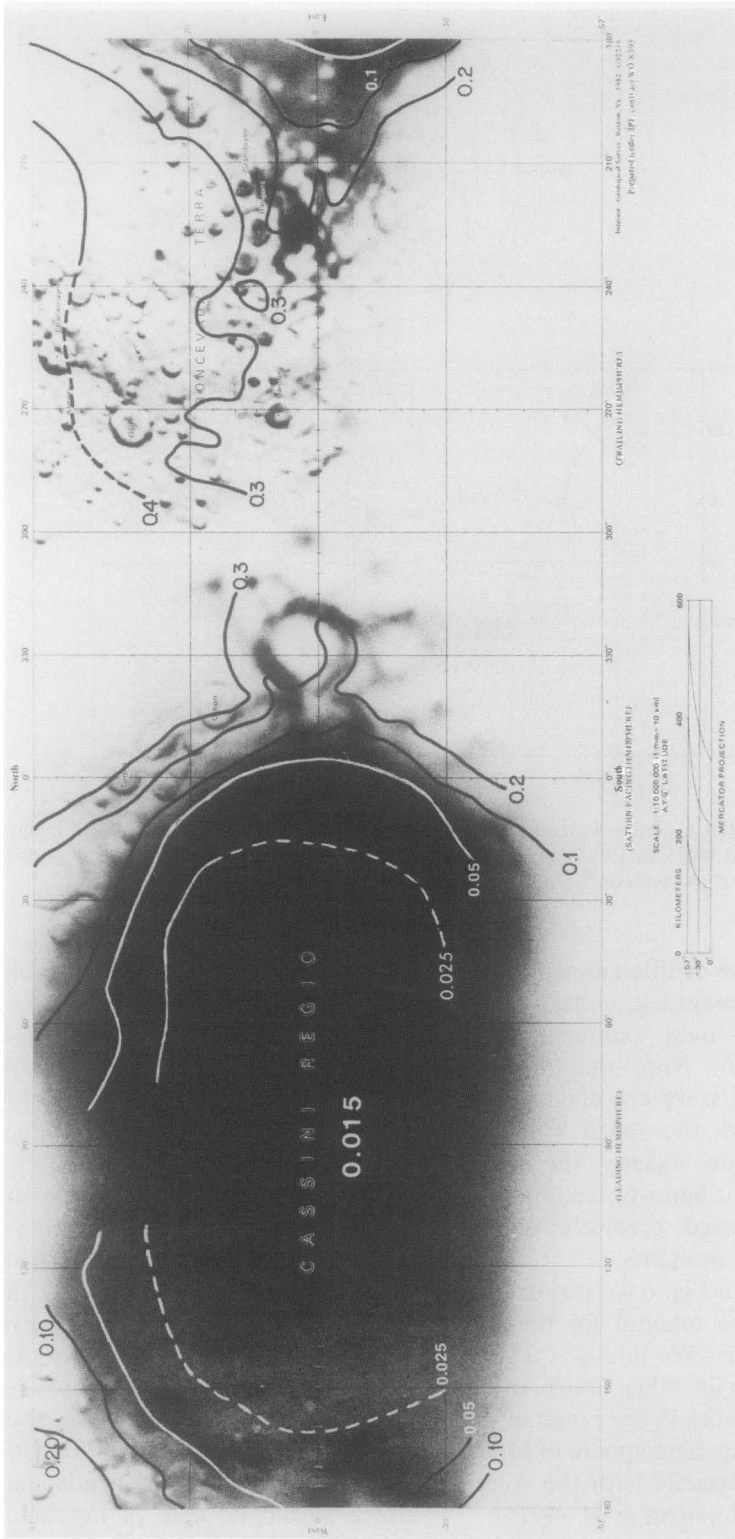


FIG. 8. Reflectance contours on Iapetus. Contours give  $f(20^\circ)/2$ . Slight mismatch between measured position of contours and location of some features on the airbrush map is probably due to the preliminary nature of airbrush map and the lack of a control net at the time of its creation.

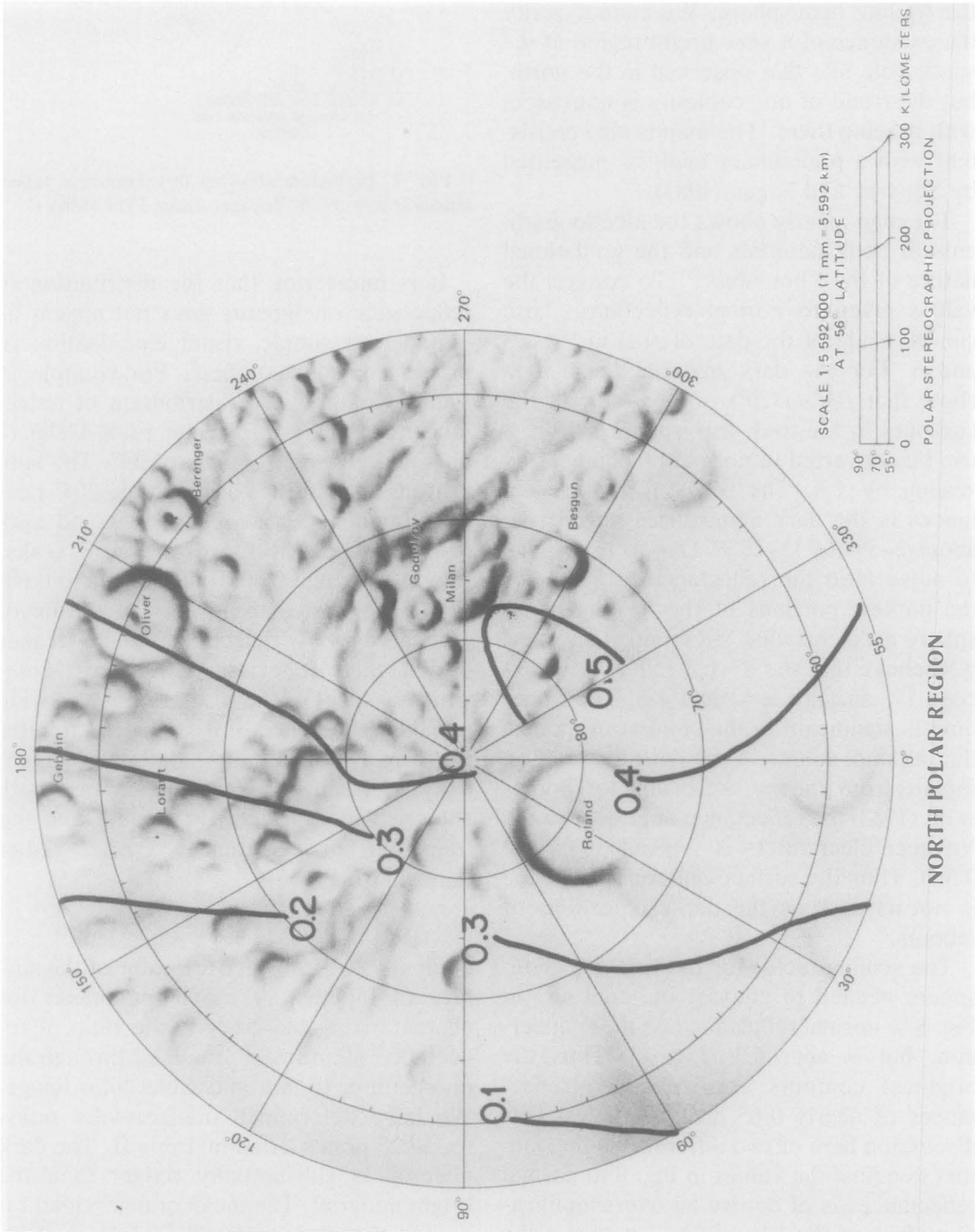


FIG. 8—Continued.

tatively similar to the one produced from Earth-based observations by Morrison *et al.* (1975), in that the north pole is bright and some dark material wraps around onto the trailing hemisphere. We cannot verify the existence of a very bright region at the south pole like that observed in the north, but the trend of our contours is consistent with it being there. The map is also consistent with a preliminary analysis presented by Squyres and Sagan (1983).

The map clearly shows the albedo gradients in both materials and the gradational nature of the "boundary." To convert the values given to normal reflectances, use can be made of the data of  $f(\alpha)$  in Figs. 3 and 6. For the dark material these data show that  $f(0^\circ)/f(20^\circ) \approx 1.6$ ; thus all the contours in the dark hemisphere in Fig. 8 can be converted to normal reflectances by scaling by 1.6. The result is that reflectances in the dark hemisphere range from about 2–3% to 15–20%. Due to low signal to noise ratio the reflectance estimate for the darkest portions of the leading hemisphere are somewhat uncertain. However, we believe that the lowest reflectances exceed 1% and are less than 4%. The upper limit is significant in the context of models that attempt to derive the dark material on Iapetus from Phoebe. According to Thomas *et al.* (1983) the reflectance of Phoebe in the Voyager clear filters is typically 0.046 to 0.060. Thus the surface material of Phoebe is not as dark as the darkest portions of Iapetus.

The scaling factor for the brighter hemisphere needed to convert the contours in Fig. 8 to normal reflectances is more uncertain, but is near 1.3 (Fig. 6). Thus the brightest contours correspond to reflectances of nearly 0.65 near the poles. Our discussion here of two different scaling factors to adjust the values in Fig. 8 to normal reflectances is of course an oversimplification. Just as the "boundary" between the bright and dark materials is gradational rather than sharp, there must also be a gradation in phase coefficient and scaling factor.

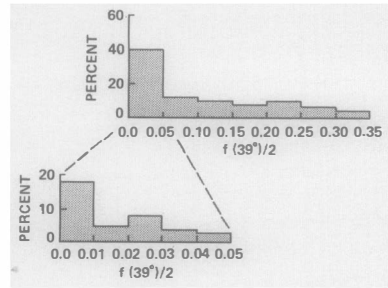


FIG. 9. Histogram showing distribution of reflectances at  $\alpha = 39^\circ$  in Voyager image FDS 43886.17.

It is interesting that the distribution of reflectance on Iapetus does not appear as bimodal as simple visual examination of processed images suggests. For example, in Fig. 9 we show the distribution of reflectances in Voyager 2 image FDS 43886.17 obtained at a phase angle of  $39^\circ$ . The sub-spacecraft point lies at longitude  $204^\circ$  near the "boundary" between bright and dark material. The reflectances in Fig. 9, scaled to  $\alpha = 0^\circ$ , range from roughly 0.02 to 0.60. While there is a strong peak in the histogram at very low reflectances and a weaker peak at high reflectances, the most noteworthy aspect of the histogram is the wide range in reflectance. It is still useful to refer to "bright" and "dark" material on Iapetus, but it must be recognized that both show a wide variation in albedo, and the transition between them is gradual rather than sharp (Fig. 8).

#### VOYAGER COLOR OBSERVATIONS

Finally, we consider the color of the surface of Iapetus. A simple parameter for characterizing the color is the ratio of reflectance in an image obtained through the orange filter to that in a violet filter image. We have determined orange/violet ratios for all 27 points listed in Table II. The dark material is substantially redder than the bright material. The mean orange/violet ratio for the dark material is  $1.45 \pm 0.10$ , while that for the bright material is  $1.25 \pm 0.04$ .

It is also important to compare the color of Iapetus to that of Phoebe. It has been

reported from Earth-based observations that while Iapetus is quite red, Phoebe is spectrally neutral (Cruikshank *et al.*, 1983). This observation is supported by Voyager color images of Phoebe, which show a disk-integrated orange/violet ratio of 1.05. If the dark material on Iapetus originated on Phoebe, it must have both become brighter and changed color substantially in the process.

#### SUMMARY

Iapetus shows variations in reflectance across its surface of a factor of 10 to 20. This is the greatest albedo range known on any object in the solar system. It is darkest at the apex of orbital motion, becomes brighter away from the apex, and is brightest near the poles. The "boundary" between bright and dark material is gradual rather than sharp. The photometric properties of the entire surface may be described adequately by a lunar-like photometric function (Eq. (1)), but the surface phase function  $f(\alpha)$  varies with albedo. These results appear consistent with those of a similar study presented recently by Goguen *et al.* (1983). The dark material on Iapetus is reddish, the bright material somewhat less so. All of Iapetus is substantially redder than Phoebe, and the darkest material on Iapetus is darker than Phoebe. This information may be used to place constraints on some of the models formulated to account for Iapetus' albedo asymmetry.

#### ACKNOWLEDGMENTS

We wish to thank Steve Gingras and Brian Hirano for their assistance in reducing the data, and Jay Goguen and R. L. Millis for helpful reviews. This work was partially supported by NASA Grant NGR 33-010-220.

#### REFERENCES

- BURATTI, B. (1983). *Photometric Properties of Europa and the Icy Satellites of Saturn*. Ph.D. thesis, Cornell University.
- BURATTI, B., AND J. VEVERKA (1983). Voyager photometry of Europa. *Icarus* **55**, 93–110.
- COOK, A. F., AND F. A. FRANKLIN (1970). An explanation of the light curve of Iapetus. *Icarus* **13**, 289–291.
- CRUIKSHANK, D. P. (1979). The surfaces and interiors of Saturn's satellites. *Rev. Geophys. Space Phys.* **17**, 165–176.
- CRUIKSHANK, D. P., J. F. BELL, M. J. GAFFEY, R. H. BROWN, R. HOWELL, C. BEERMAN, AND M. ROGNSTAD (1983). The dark side of Iapetus. *Icarus* **53**, 90–104.
- DANIELSON, G. E., P. N. KUPFERMAN, T. V. JOHNSON, AND L. A. SODERBLUM (1981). Radiometric performance of the Voyager cameras. *J. Geophys. Res.* **86**, 8683–8690.
- GOGUEN, J., M. TRIPPICO, AND D. MORRISON (1983). Voyager feature-fixed photometry of the surface of Iapetus. *Bull. Amer. Astron. Soc.* **15**, 855 (abstract).
- HAPKE, B. W. (1963). A theoretical photometric function for the lunar surface. *J. Geophys. Res.* **68**, 4571–4586.
- IRVINE, W. M. (1966). The shadowing effect in diffuse reflection. *J. Geophys. Res.* **71**, 2931–2937.
- KLAASEN, K. P., T. C. DUXBURY, AND J. VEVERKA (1979). Photometry of Phobos and Deimos from Viking orbiter images. *J. Geophys. Res.* **84**, 3478–3486.
- MORRISON, D., T. J. JONES, D. P. CRUIKSHANK, AND R. E. MURPHY (1975). The two faces of Iapetus. *Icarus* **24**, 157–171.
- MORRISON, D. (1977). Radiometry of satellites and of the rings of Saturn. In *Planetary Satellites* (J. A. Burns, Ed.), pp. 269–301. Univ. of Arizona Press, Tucson.
- NOLAND, M., AND J. VEVERKA (1977a). The photometric functions of Phobos and Deimos. II. Surface photometry of Deimos. *Icarus* **30**, 200–211.
- NOLAND, M., AND J. VEVERKA (1977b). The photometric functions of Phobos and Deimos. III. Surface photometry of Phobos. *Icarus* **30**, 212–223.
- SMITH, B. A., AND Voyager Imaging Team (1981). Encounter with Saturn: Voyager I imaging science results. *Science* **212**, 163–191.
- SOTER, S. (1974). Paper presented at IAU Planetary Satellites Conference, Cornell University.
- SQUYRES, S. W., AND J. VEVERKA (1981). Voyager photometry of Ganymede and Callisto. *Icarus* **46**, 137–155.
- SQUYRES, S. W., AND C. SAGAN (1983). Albedo asymmetry of Iapetus. *Nature* **303**, 782–785.
- THOMAS, P., J. VEVERKA, M. DAVIES, D. MORRISON, AND T. V. JOHNSON (1983). Phoebe: Voyager 2 observations. *J. Geophys. Res.* **88**, 8736–8742.